

On the Sound Radiation From a Circular Hatchway

Jorge P. Arenas

Institute of Acoustics, University Austral of Chile, Valdivia, Chile

Low-frequency sound radiation from vibrating plates is a practical problem often found in engineering applications. In this article, the sound radiation from a circular hatchway is examined using a discrete approach based in the acoustic resistance matrix. Since this matrix can be combined with the volume velocity vector on the discretized vibrating circular surface, the sound radiation efficiency can be estimated through matrix approaches. The limitation of the approach is discussed by using benchmark results presented in previous works. The method produces acceptable results in low frequencies when the response of the plate is dominated by one low structural mode. When the response of more than one mode is significant, the method gives good estimation of the total sound power just for frequencies up to the first resonance. However, the method can be applied to complex and irregular vibrating plane surfaces.

low-frequency noise sound radiation circular plate hatchway

1. INTRODUCTION

Low-frequency sound radiation from vibrating structures can produce exposure of workers to noise levels that involve a risk of both auditory and nonauditory health effects. In addition, low-frequency noise of high intensity might cause damage to other adjacent structures. In particular, the vibration of a plate and its interaction with the surrounding fluid medium will result in a coupled problem involving radiation of noise. Since circular plates are commonly found in engineering applications, there is a large body of research on the modeling and engineering design of circular plates [1, 2]. In particular, there have been many studies on predicting the sound power radiated from a circular plate [3]. In a recent article, Rdzanek, Rdzanek, Engel, et al. reported a motivating study on the modal low-frequency noise generated by a vibrating elastically supported circular plate embedded into a flat infinite baffle [4]. Their approach allows one to estimate the low-frequency sound power radiated from both axisymmetric and asymmetric modes, and virtually

for any uniform boundary condition at the contour of the plate. They applied the technique to some hatchway covers mounted on a ship deck as a particular example of such a circular plate. In this article, a different approach is presented to analyze the same problem. The approach is based on the acoustic radiation resistance matrix and it is completely discrete in nature, so it can be readily implemented into computer codes. In previous works, this method was used to estimate sound radiation efficiency of rectangular plates [5]. Using Rdzanek et al.'s examples as benchmark results, the limitations of the discrete technique are discussed and the advantages of Rdzanek et al.'s approach become more evident.

2. BASIC EQUATIONS

2.1. Transverse Vibration of a Circular Plate

Leissa [6] and Meirovitch [7] give the equation of motion for the small displacement $w(r, \varphi, t)$ of a

This work was supported by Fondecyt 1060117.

Correspondence and requests for offprints should be sent to Jorge P. Arenas, Institute of Acoustics, Edif. 6000, Campus Miraflores, Univ. Austral de Chile, Casilla 567, Valdivia, Chile. E-mail: <jparenas@uach.cl>.

thin, isotropic circular plate of radius a , which is excited by a force $f(r, \varphi, t)$:

$$D\nabla^4 w + \rho h \frac{\partial^2 w}{\partial t^2} = f(r, \varphi, t), \quad (1)$$

where ρ —density of the plate, h —thickness, $D = Eh^3/12(1 - \nu^2)$ —bending stiffness of the plate, E —its Young’s modulus, ν —its Poisson ratio, and ∇^4 —the square of the Laplacian operator in polar co-ordinates. If the plate is excited by a time-harmonic point force of circular frequency ω , at locations $r = a_0$ and $\varphi = \varphi_0$,

$$f(r, \varphi, t) = \frac{F_0 e^{j\omega t}}{r} \delta(r - a_0) \delta(\varphi - \varphi_0), \quad (2)$$

where F_0 —force amplitude of the excitation.

Assuming time-harmonic solution of Equation 1, i.e., $w(r, \varphi, t) = W(r, \varphi) e^{j\omega t}$, and following Rdzanek et al.’s [4] notation, the forced harmonic response of the plate can be written as the modal superposition

$$W(r, \varphi) = \sum_{m=0}^{\infty} \sum_{n=1}^{\infty} [c_{mn}^{(c)} W_{mn}^{(c)} + c_{mn}^{(s)} W_{mn}^{(s)}], \quad (3)$$

where $W_{mn}^{(c)} = W_{mn}(r) \cos m\varphi$, $W_{mn}^{(s)} = W_{mn}(r) \sin m\varphi$,

$$W_{mn}(r) = A_{mn} [J_m(k_{mn}r) + C_{mn} I_m(k_{mn}r)], \quad (4)$$

J_m, I_m — m th order Bessel and modified Bessel functions, respectively,

$$k_{mn}^4 = \omega_{mn}^2 \rho h / D, \quad (5)$$

ω_{mn} —corresponding eigenfrequency of mode (m, n) ,

$$c_{mn}^{(c)} = \frac{F_0}{\pi \rho \omega^2 h a^2} \frac{W_{mn}(a_0) \cos m\varphi_0}{(k_{mn} / k_D)^4 - 1}, \quad (6)$$

$$c_{mn}^{(s)} = \frac{F_0}{\pi \rho \omega^2 h a^2} \frac{W_{mn}(a_0) \sin m\varphi_0}{(k_{mn} / k_D)^4 - 1}$$

and $k_D^4 = \omega^2 \rho h / D$ is the structural wavenumber. The constants A_{mn} and C_{mn} in Equation 4 are determined from the boundary conditions of the circular plate. In Equations 6, the internal damping loss factor of the plate has been neglected.

Uniform boundary conditions at the contour of the plate are expressed with Equations 7–8 [6]:

$$M_r(a, \varphi) = K_\psi \frac{\partial W}{\partial r}(a, \varphi), \quad (7)$$

$$V_r(a, \varphi) = -K_w W(a, \varphi), \quad (8)$$

where M_r —bending moment of the plate’s edge, V_r —force resisting transverse deflection of the plate edge, and K_ψ, K_w —corresponding distributed boundary stiffness values. Dimensionless boundary stiffness values are defined as $q = K_w a^3 / D$ and $p = K_\psi a / D$. Frequency equation for the problem is obtained by substituting the solution of Equation 1 with $f(r, \varphi, t) = 0$ (free vibrations),

$$W_{mn}(r, \varphi) = \begin{cases} \cos m\varphi \\ \sin m\varphi \end{cases} W_{mn}(r), \quad (9)$$

into Equations 7–8 (see Equation 11 in Rdzanek et al. [4]). The values at which a resonance of mode (m, n) takes place are given with the eigenvalue $\lambda_{mn} = k_{mn} a$. Therefore, the time-harmonic normal velocity of mode (m, n) on the surface of the plate is given with $V_{mn}(r, \varphi) = j\omega_{mn} W_{mn}(r, \varphi)$.

Equation 3 can be written in matrix form by truncating the infinite series to a finite value of $m = M$ and $n = N$. Therefore,

$$W(r, \varphi) = \mathbf{c}^T \mathbf{\Phi} \mathbf{b}, \quad (10)$$

where \mathbf{c} —column vector of length $M + 1$ whose elements are $\cos m(\varphi - \varphi_0)$, \mathbf{b} —column vector of length N whose elements are all ones, and $\mathbf{\Phi}$ — $M + 1 \times N$ matrix whose elements are

$$\Phi_{mn} = \frac{W_{mn}(r) W_{mn}(a_0)}{(k_{mn} / k_D)^4 - 1}. \quad (11)$$

2.2. Sound Power Radiated

Considering that the circular plate is mounted flush into an infinite baffle and that the vibrating plate surface is divided into N' small elements of area S_k , with $k = 1, 2, \dots, N'$, the local specific acoustic radiation impedance can be estimated on the surface as

$$Z_{ik} = p_i / V_k, \quad (12)$$

where p_i —sound pressure amplitude at point i due to a point source located at point k , and normal velocity V_k .

If we assume that the characteristic length of the surface elements is small compared to a typical acoustic wavelength, the pressure and velocity can be considered constant over each

element and can be represented by an average value. Therefore, Equation 12 can be written as

$$Z_{ik} = p_i / u_k, \tag{12}$$

where $u_k = \int V_k dS_k$ is the volume velocity at point k . Therefore, using the reciprocity principle and the definition of sound power, it can be shown that the average sound power can be estimated by Arenas and Crocker [5]:

$$\Pi = \frac{1}{2} \mathbf{u}^H \mathbf{R} \mathbf{u}, \tag{13}$$

where \mathbf{u} — $N' \times 1$ column vector of volume velocities, \mathbf{H} —Hermitian, and \mathbf{R} —symmetric $N' \times N'$ acoustic resistance matrix whose elements are given by the real part of Equation 12.

An approximate low-frequency formula for calculating the elements of \mathbf{R} when fluid loading is neglected is given by Berkhoff [8]:

$$R_{ik} = \begin{cases} \frac{\rho_0 c k^2}{2\pi} & i = k \\ \frac{\rho_0 c k}{2\pi d} \sin kd & i \neq k \end{cases}, \tag{14}$$

where ρ_0 —density of the fluid, c —speed of sound, k —wavenumber of the sound, and d —distance between the center points of elements i and k . An important observation is that \mathbf{R} depends neither on the velocity distribution on the plate nor on the boundary conditions. Therefore, computation of \mathbf{R} is needed just once per frequency and, consequently, data can be stored for reusing, reducing the computational cost.

Now, the sound radiation efficiency is

$$\sigma = \frac{\Pi}{\rho_0 c S \langle V^2 \rangle}, \tag{15}$$

where S —total surface of the plate and $\langle V^2 \rangle$ —space-averaged mean square normal vibration velocity amplitude, defined as

$$\langle V^2 \rangle = \frac{1}{2S} \int_S |V|^2 dS. \tag{16}$$

In the rest of this paper, when the sound radiation is produced by a single mode (m, n) the sound radiation efficiency will be denoted as σ_{mn} .

2.3. Discretization of a Circular Plate

Implementation of the computational codes requires partition of the total surface of the circular plate into small elements of equal area. However, transformation to a classical polar coordinate system will produce surface elements of different area. Therefore, to discretize a circular surface of radius a , into small elements of equal area, the surface is divided first into L equally spaced concentric rings [9]. Thus, the co-ordinates of the center point of each element are $r_i = a(2i - 1)/2L$ and $\varphi_i = \pi(2i - 1)/4(2i - 1)$, where $i = 1, 2, \dots, L$ and $j = 1, 2, \dots, 4(2i - 1)$. This discretization produces a total of $4L^2$ elements having a surface $\Delta S = \pi(a/L)^2/4$. An example using $L = 10$ is shown in Figure 1.

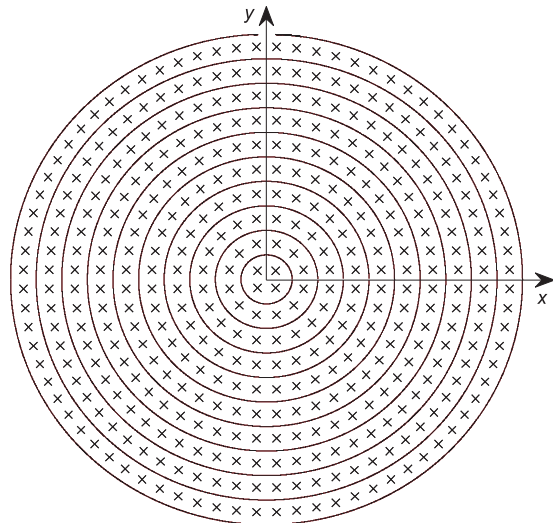


Figure 1. Example of a discretization of a circular surface into small elements of equal area. The center point of each discrete element is indicated by a cross.

On the other hand, Equation 16 can be estimated with

$$\langle V^2 \rangle = \frac{4L^2}{2\pi^2 a^4} \sum_{j=1}^{4L^2} |u_j|^2 = \frac{2L^2}{\pi^2 a^4} \mathbf{u}^H \mathbf{u}. \tag{17}$$

3. NUMERICAL EXAMPLES

In this section some numerical examples of circular plates are presented. All the computations were performed using programs written in Matlab® version 7.1. In addition, it has been assumed that the circular baffled plate is

radiating sound into air ($\rho_0 = 1.21 \text{ kg/m}^3$), so the plate response is not significantly affected by the surrounding environment.

In Rdzanek et al. [4] an exact integral expression for the sound radiation efficiency related to the mode (m, n) is derived from its Hankel representation (see Equation 21 of Rdzanek et al.). Evidently, sound radiation efficiency may be dependent on the particular boundary condition at the edge of the circular plate, which can be defined through the appropriate values of p and q . An interesting result is to plot the sound radiation efficiency of some fundamental modes for some classical boundary conditions. Figure 2 shows the results of sound radiation efficiency of the lowest structural modes of a circular plate of radius $a = 0.3 \text{ m}$ and thickness $h = 6 \times 10^{-3} \text{ m}$, made of steel ($E = 210 \text{ GPa}$, $\nu = 0.3$, $\rho = 7850 \text{ kg/m}^3$) which is clamped ($p = \infty$ and $q = \infty$), simply-supported ($p = 0$ and $q = \infty$), free ($p = 0$ and $q = 0$), and guided ($p = \infty$ and $q = 0$). In computing the results shown in Figure 2, the exact integral representation has been used. For making a comparison, sound radiation is plotted as a function of the dimensionless ratio ff_c , where f_c is the critical frequency of the plate. The critical frequency is defined as the frequency at

which the propagation speed of the bending wave in the plate is equal to the speed of sound in the air ($c = 343 \text{ m/s}$).

The results are quite similar to those obtained for square plates [5]. As expected, the radiation efficiency approaches unity for frequencies at and above f_c . It should also be noted that well below the critical frequency, the radiation efficiency is larger in the case of a simply-supported plate but the difference is slightly over 1 dB. Similar observation can be made from previous works on rectangular plates [10], where in the low-frequency range plates with edges that are more constrained do not always have larger radiation efficiencies than plates with edges that are less constrained. However, there is a significant difference in sound radiation efficiency for guided and free circular plates. For very low frequencies, a clamped circular plate could have a radiation efficiency which is more than 50 dB greater than that of a free plate.

Figures 3–4 show the results of the modal radiation efficiency for some structural modes of a circular plate having a uniform elastic boundary condition defined by $q = 10$ and $p = 100$. The modal radiation efficiencies were calculated using the acoustic resistance matrix

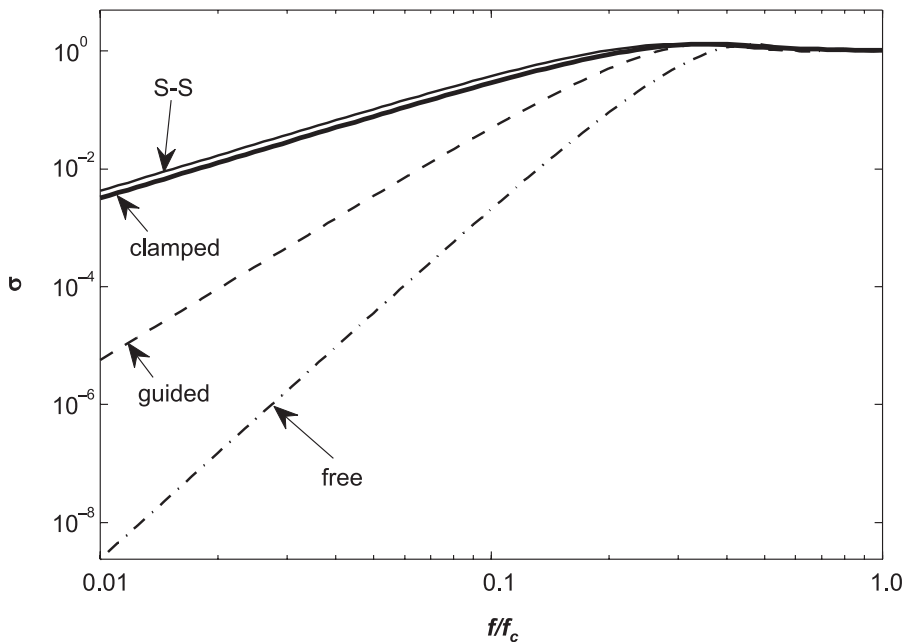


Figure 2. Radiation efficiency (σ) of the lowest mode of a simply-supported (S-S), clamped, guided, and free circular plate as a function of f/f_c .

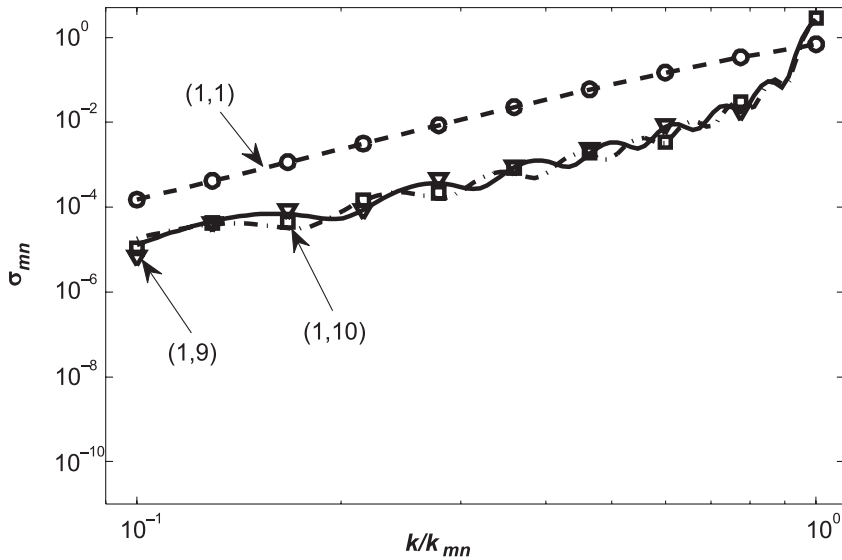


Figure 3. Radiation efficiency (σ_{mn}) for a number of modes of a circular plate of $q = 10$ and $p = 100$. Symbols indicate the exact integral values.

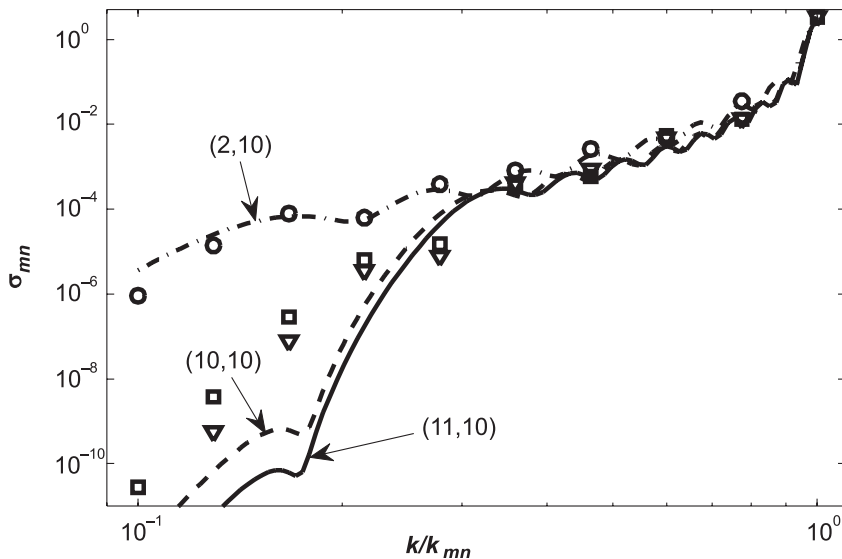


Figure 4. Radiation efficiency (σ_{mn}) for a number of modes of a circular plate of $q = 10$ and $p = 100$. Symbols indicate the exact integral values.

(Equations 13–16) and they are plotted as a function of the dimensionless ratio k/k_{mn} . A number $L = 20$ was used in the discretization. For comparison, modal radiation efficiencies were also computed using the exact integral representation and they are displayed as symbols in the same plot. There is good agreement with the curves presented in the literature (Figure 1 of Rdzaneck et al. [4]) for those modes having λ_{mn} lower than ~ 30 . The low frequency estimation deteriorates for modes (10, 10) and (11, 10) which have $\lambda_{mn} = 43.4$ and $\lambda_{mn} = 44.8$, respectively. It is

clear that for frequencies well below $k = k_{mn}$, the efficiency of mode (1,1) is large compared with the efficiencies of all the other modes.

Although the acoustic resistance matrix method does not consider the intermodal efficiency, the total sound power radiated from a circular plate can be estimated for very low frequencies using Equation 15 and 17. From Equation 15 we obtain

$$\Pi = \rho_0 c S \sigma \langle V^2 \rangle. \tag{18}$$

Now, for frequencies below the first resonance, σ can be approximated by $4Sf^2/c^2$ [11], where f is

the frequency ($\omega/2\pi$). Above the first resonance and up to $3c/P$, where P is the perimeter of the plate, there are formulae for certain particular boundary conditions, and it is well-known that for a simply-supported square plate, $\sigma = 4\pi^2 D/c^2 S \rho_s$, where ρ_s is the plate surface density. The space-averaged mean square normal vibration velocity amplitude may be estimated using Equation 17.

As an example, Rdzanek et al.'s [4] application of a circular hatchway is computed using Equation 18 for a uniform elastic boundary condition defined again by $q = 10$ and $p = 100$. It is assumed that the hatchway covers are made of three different materials: polystyrene ($E = 3.6$ GPa, $\nu = 0.24$, $\rho = 1050$ kg/m³), hardened glass ($E = 72$ GPa, $\nu = 0.24$, $\rho = 2900$ kg/m³), and steel ($E = 210$ GPa, $\nu = 0.3$, $\rho = 7850$ kg/m³). The radius of the plate is $a = 0.3$ m and the thickness is $h = 6 \times 10^{-3}$ m. The final aim of the example was to select the hatchway cover that produces the lowest sound power level when the hatchway is subject to an harmonic force applied at $a_0 = 0.15$ m (to assure its asymmetric excitation) whose amplitude is $F_0 = 25 \pi a^2$ N. Computation of the normal velocity vectors is made through the matrix Equation 10. Since Equation 10 can be efficiently computed using Matlab[®], a large number of modes can be considered in the estimation. In this case,

$M = N = 11$. For computing the sound power at frequencies above the first resonance, the expression for an equivalent simply-supported square plate has been used. Figure 5 shows the results of sound power level as a function of ka of the circular hatchway.

Although it is difficult to make a direct comparison with the results presented in Rdzanek et al.'s Figure 4 [4] because there is a plotting error in the dimensionless frequency axis, some tendencies can be observed. Obviously, the sound power radiated from the hatchway reaches high levels at resonance. If we divide the axis scale of Rdzanek et al.'s Figure 4 by 20, we get quite similar results for frequencies up to the first resonance of each sample plate. The results are not as good for frequencies above the first resonance, where the effect of intermodal efficiency might be important. It seems that the matrix approach underestimates the sound power radiated above the first resonance. Here, Rdzanek et al.'s method becomes quite powerful and efficient. However, the discrete method allows one to select the most silent plate (the one made of steel) for frequencies such that $ka < 0.15$, where the sound power level is lower than 40 dB. Some authors have suggested that for plates radiating under light fluid loading the influence of intermodal radiation may be neglected and, to

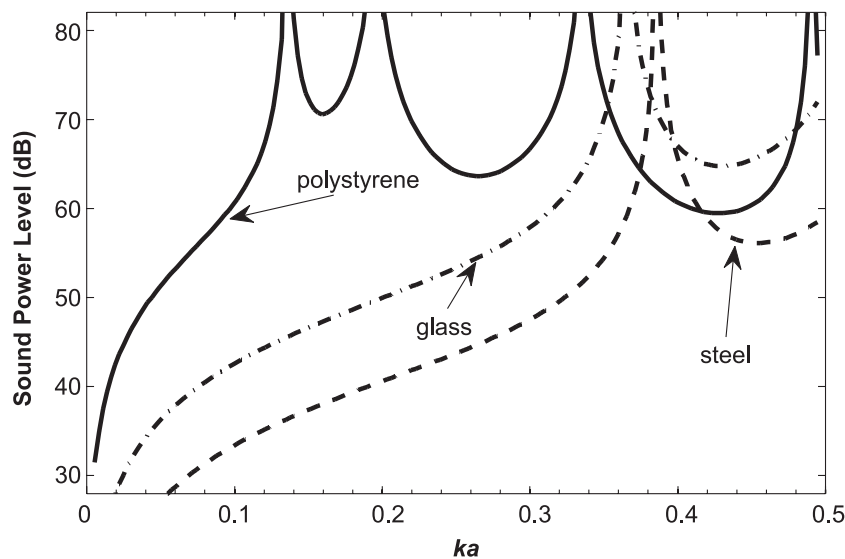


Figure 5. Results of the total sound power level ($\Pi_{\text{ref}} = 10^{-12}$ W) for some sample hatchway covers.

a first approximation, the radiated sound power of a plate is the sum of the power radiated by each mode separately [12]. However, according to Rdzanek et al.'s results, this is not true in this case for frequencies above the first resonance. Clearly, the matrix approach could give better results for higher frequencies, although its applicability will be limited by the number of discrete elements.

4. CONCLUDING REMARKS

A discrete approach to study the low-frequency sound radiation from a circular hatchway has been presented. From comparison with some benchmark results reported in the literature, we observe that the discrete method works fine in the low-frequency range when the response of the plate is dominated by one mode, i.e., at resonance. When the response of more than one mode is significant, the method gives good estimation of the sound radiation for frequencies up to the first resonance. Above that frequency, Rdzanek et al.'s [4] method appears more convenient for numerical computations. However, despite the limitations, the discrete method could be combined with other numerical methods, such as finite elements, to estimate the sound radiation from complex and irregular plane surfaces.

REFERENCES

1. Bauer HF, Eidel W. Determination of the lower natural frequencies of circular plates with mixed boundary conditions. *J Sound Vib.* 2006;292:742–64.
2. Bauer HF, Eidel W. Transverse vibration and stability of spinning circular plates of constant thickness and different boundary conditions. *J Sound Vib.* 2007;300:877–95.
3. Rdzanek WP, Engel Z, Rdzanek W. Theoretical analysis of sound radiation of an elastically supported circular plate. *J Sound Vib.* 2003;265:155–74.
4. Rdzanek WP, Rdzanek WJ, Engel Z, Szemela K. The modal low frequency noise of an elastically supported circular plate. *International Journal of Occupational Safety and Ergonomics (JOSE).* 2007;13:147–57.
5. Arenas JP, Crocker MJ. Sound radiation efficiency of a baffled rectangular plate excited by harmonic point forces using its surface resistance matrix. *Int J Acoust Vib.* 2002;7:217–29.
6. Leissa A. *Vibration of plates.* New York, NY, USA: Acoustical Society of America; 1993.
7. Meirovitch L. *Analytical methods in vibration.* New York, NY, USA: MacMillan; 1967.
8. Berkhoff AP. Sensor scheme design for active structural acoustic control. *J Acoust Soc Am.* 2000;108:1037–45.
9. Arenas JP. Numerical computation of the sound radiation from a planar baffled vibrating surface. *J Comp Acoust.* 2008; 16:321–41.
10. Gomperts MC. Sound radiation from baffled, thin, rectangular plates. *Acustica.* 1977;37:93–102.
11. Xie G, Thompson DJ, Jones CJC. The radiation efficiency of baffled plates and strips. *J Sound Vib.* 2005;280:181–209.
12. Guyader JL. Sound radiation from structures and their response to sound. In: Crocker MJ, editor. *Handbook of noise and vibration control.* Hoboken, NJ, USA: Wiley; 2007. p. 79–100.